

Measurement and modelling of residual stress in wire-feed additively manufactured titanium

Bilal Ahmad, Sjoerd O. van der Veen, Michael E. Fitzpatrick, Hua Guo

Author post-print (accepted) deposited by Coventry University's Repository

Original citation & hyperlink:

Ahmed, B, van der Veen, S, Fitzpatrick, M & Guo, H 2018, 'Measurement and Modelling of Residual Stress in Wire-Feed Additively Manufactured Titanium' Materials Science and Technology, vol. 34, no. 18, pp. 2250-2259.

<https://doi.org/10.1080/02670836.2018.1528747>

DOI 10.1080/02670836.2018.1528747

ISSN 0267-0836

ESSN 1743-2847

Publisher: Taylor and Francis

This is an Accepted Manuscript of an article published by Taylor & Francis in Materials Science and Technology on 03 October 2018, available online: <http://www.tandfonline.com/10.1080/02670836.2018.1528747>

Copyright © and Moral Rights are retained by the author(s) and/ or other copyright owners. A copy can be downloaded for personal non-commercial research or study, without prior permission or charge. This item cannot be reproduced or quoted extensively from without first obtaining permission in writing from the copyright holder(s). The content must not be changed in any way or sold commercially in any format or medium without the formal permission of the copyright holders.

This document is the author's post-print version, incorporating any revisions agreed during the peer-review process. Some differences between the published version and this version may remain and you are advised to consult the published version if you wish to cite from it.

Measurement and Modelling of Residual Stress in Wire-Feed Additively Manufactured Titanium

*Bilal Ahmad^{1, a}, Sjoerd O. van der Veen^{2, b}, Michael E. Fitzpatrick^{1, c}, Hua Guo^{1, d}

¹*Faculty of Engineering, Environment and Computing, Coventry University, Gulson Road, Coventry, CV1 2JH, UK*

²*Airbus Operations SAS, 316 route de Bayonne, Toulouse, France*

^aac2333@coventry.ac.uk, Tel: +44 2477 657734

^bsjoerd.van-der-veen@airbus.com, Tel: +33 5 67 19 69 62

^cmichael.fitzpatrick@coventry.ac.uk, Tel: +44 2477 685673

^dhua.guo@coventry.ac.uk, Tel: +44 2477 659595

* Corresponding author

Measurement and Modelling of Residual Stress in Wire-Feed Additively Manufactured Titanium

Residual stresses were characterized in a wire-feed additively manufactured titanium alloy component. A numerical simulation based on the inherent strain method was used to model residual stresses arising from the manufacturing process. The contour method was used to experimentally determine the residual stress field. High tensile residual stresses were seen at and around the interface of the substrate and the deposited metal. Compressive residual stresses were present in the substrate and at the top of the deposit. Satisfactory correlation was achieved between the results from the numerical simulation and the contour method, except for the location of the root of the deposit. The effect of preheating the sample substrate on the residual stress distribution is also discussed. Keywords: wire feed additive manufacturing; residual stress; inherent strain-based method; contour method; titanium.

Introduction

The wire-feed additive manufacturing (WFAM) process is particularly attractive for aerospace industry due to the high cost of titanium [1] as well as the high cost of machining it. With WFAM near-to-net shape preforms can be made [2], which then require less machining to reach the desired final geometry. Little material has to be recycled and less time is spent in machining. The fatigue properties of WFAM titanium in certain cases have outperformed the traditional processes [3].

In wire-feed additive manufacturing, the wire is made of materials such as titanium, aluminium, stainless steel, etc., and is deposited on a substrate with the use of a heat source such as a laser, arc, or electron beam [4]. The process is somewhat similar to the arc welding processes [5]. The substrate can be made of the same or a different material as that being deposited. The part is built by depositing the melted layers successively onto the previous layers. The wire feed system has a high deposition rate [6], therefore it is particularly suitable for the production of large components [4,7]. Wire feed additive manufacturing has been used to develop large aerospace parts [8]. The various parameters of the WFAM process include deposit speed, wire feed rate, applied energy, deposit sequence, etc. [5]. During the build-up process each metal layer undergoes a cycle of heating and cooling [9]. Shrinkage of the deposit during the solidification process is the main cause of the generation of residual stress. Tensile

residual stress is usually highest in the build longitudinal direction [8], and unclamping the sample after the WFAM causes high tensile residual stress at the interface of the substrate and deposit, as well as compressive residual stress at the top of the deposit [7]. Various procedures such as preheating of the substrate, inter-pass cooling of the deposit, inter-pass rolling [10], etc., are being developed for the WFAM process to minimize the induced residual stresses [7].

WFAM differs from conventional welding as a large amount of heat is input to the part compared to the small initial mass of the part. Also a large number of passes are made by the heat-source. This situation then leads to gradual warming of the part, which may have a non-negligible impact on the final residual stresses. Coupled thermo-mechanical finite element simulation has been predominantly used to predict the shrinkage and residual stress generated in wire feed additive manufacturing. Relevant literature from the field of welding as well as a method to adapt these modelling principles to WFAM can be found in [11]. Even weakly-coupled thermo-mechanical simulations usually take a long run-time, for example for the prediction of residual stress in an industrial-size WFAM part. In the present study an inherent-strain-based method was used to simulate WFAM because of its high solving speed compared to the coupled thermo-mechanical simulations. The inherent strain method was first used to analyse the residual stress in the welded structures [12], and was applied to a number of cases thereafter [13,14]. Numerical simulation based on inherent strain reduces the computational effort compared to even weakly-coupled thermo-mechanical simulations, and was therefore selected for the present work. This numerical simulation approach has been extended to predict the residual stresses in selective-laser-melting additively manufactured titanium (Ti-6Al-4V) and Inconel 718: further details can be found in [15]. In that study a good correlation was achieved between the numerical simulation (inherent strain-based method) and the contour method results.

Residual stress in electron beam additive manufacturing, a type of WFAM, has been previously predicted with the thermo-mechanical simulation [16]; however for large WFAM components little work is available in the literature on the analysis of residual stress. In this paper the longitudinal stress component of the WFAM titanium (Ti-6Al-

4V) sample was measured at its centre location with the contour method. The contour method results were correlated with the results of the numerical simulation.

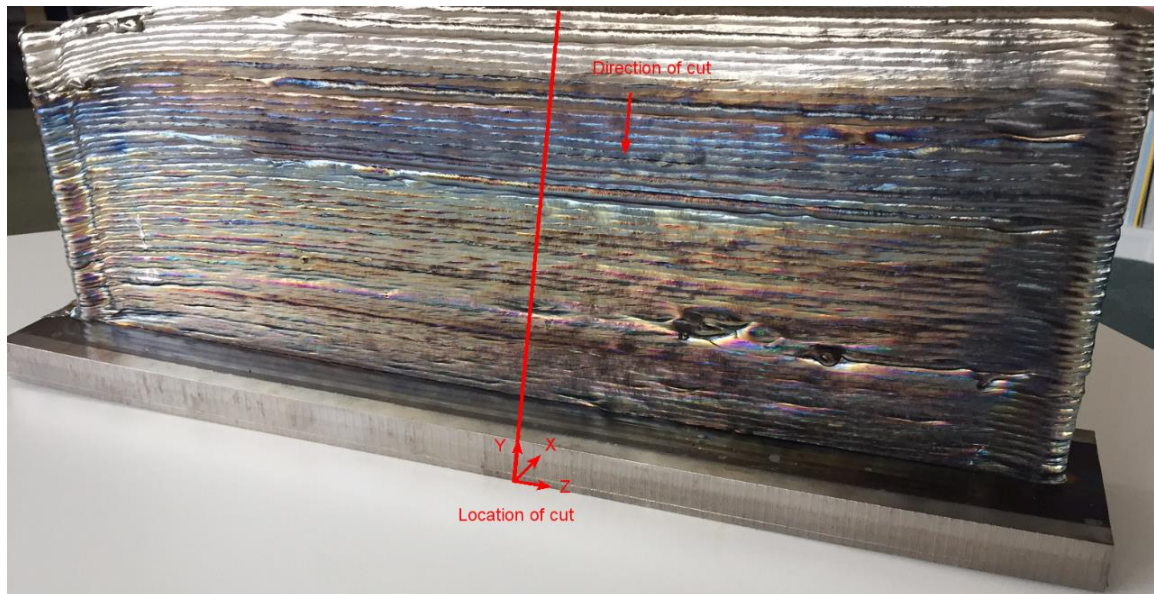
The contour method is a destructive technique for determination of residual stress, which is based on stress relaxation. In the contour method a part is cut into two halves, and the stress component normal to the cut surface is determined [17]. Wire electro-discharge machining (WEDM) is used to cut the component in which the stress state is to be determined. It is assumed for the cutting stage that the cut surface is flat and no new stresses are incorporated. Following the cutting stage, both cut surfaces/halves are measured with a co-ordinate measuring machine (CMM). Then data analysis is carried out to clean and smooth the measured displacement data, and to average the data from the two surfaces. Finally a three-dimensional finite element (FE) model of one of the cut surfaces is built, and the reverse of the measured contour is applied as the displacement boundary conditions. Constraints are applied to the model to avoid rigid body motion. A linear-elastic FE analysis is then used to back-calculate the residual stress in the sample that existed before the cut was made [17].

During the sample cutting stage errors can be incorporated in to calculated results, which however can be minimized: *e.g.*, roughness can be improved by using short spark pulse durations [18], and where necessary a data correction helps to improve the estimated stress results [19,20]. Various approaches have been developed to minimize errors in the application of the contour method [21,22].

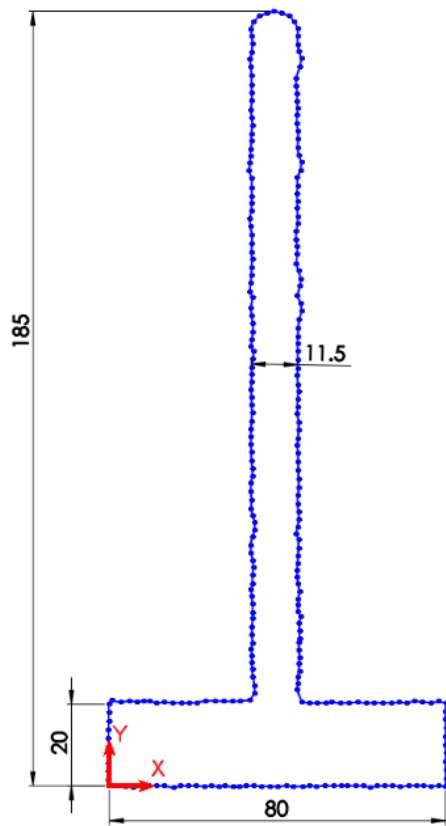
The contour method provides a full two-dimensional and through-thickness residual stress map. It is insensitive to material microstructure. Other residual stress measurement techniques such as X-ray diffraction and incremental centre-hole drilling are applicable only for near-surface stresses. These techniques require the samples to be smooth and of good surface finish. Neutron diffraction can measure the through thickness residual stresses up to a certain depth in the sample; however it is significantly affected by sample positioning, neutron beam path length in the sample, and texture. With few specialised neutron facilities around the world, obtaining the beam time is a competitive process. In-addition to this long measurement times due to weak scattering means that relatively data for few measurement points can be obtained. As a result, the contour method has become popular and widespread, and has been applied to a wide range of materials and processing methods [23,24].

Materials and methods

An electron-beam additively manufactured titanium (Ti-6Al-4V) sample was fabricated by Sciaky, Inc. Figure 1(a) shows a photo of the sample. The length of the deposit and substrate were 450 mm and 490 mm respectively. The sample was measured in the as-deposited form. The substrate and deposit both were made of titanium (Ti-6Al-4V) alloy, and the substrate was pre-heated before the deposition. The sample suffered from distortion when unclamped after the metal deposition. The longitudinal distortion at the outer most edges of the substrate was about 3 mm. For contour method measurement the WEDM cut was made at the mid location of the sample (as marked on Figure 1a) to obtain the longitudinal stress component. The longitudinal stress component was expected to be of the highest magnitude for the wire feed additive manufacturing process. The dimensions of the measured cross-section after the WEDM cut are shown in Figure 1(b).



(a)



(b)

Figure 1. Wire feed additively manufactured titanium (Ti-6Al-4V) sample (a) Photo; & (b) Dimensions of the sample cut surface (all dimensions are in mm) During WFAM heavy steel clamps were used to prevent the movement of the substrate. Figure 2 shows a schematic of the clamping arrangement used during the additive manufacturing.

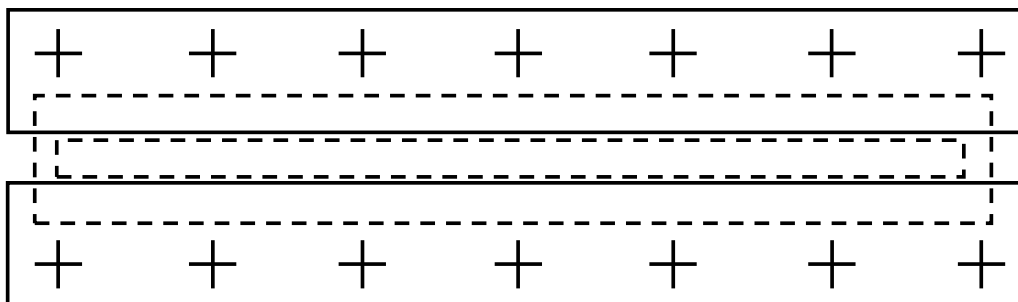


Figure 2. Schematic of clamping arrangement used during additive manufacturing

Prior to the actual contour cut the WEDM cutting parameters were tested by a small cut at one end of the sample. Low-power cutting parameters for the sample size and the geometry were used. Not much literature is available to-date for the selection of the

WEDM parameters for the contour method. Reference [17] however recommends to use the WEDM skim cut parameters. The machine low-power cutting settings provide low values for the important electrical parameters like pulse duration [18,20], voltage, and current. The low-power cutting parameters enhance the surface finish of the cut parts, as well as tending to reduce the magnitude of any cutting artefacts. The following values for these parameters were used:

VM (machining voltage) = 8 V; CC (current) = 1 A; ON (pulse duration time) = 1 μ s.

The use of sacrificial layers is considered beneficial to avoid the effect of the cutting artefacts for the very-near-surface stresses. However, a number of restrictions may limit the use of sacrificial layers: *e.g.*, for large samples, irregular surfaces and shapes/geometries, electrical conductivity of the epoxy used, etc. The sample was cut on a Fanuc Robocut α -C600i WEDM. A 0.25-mm-diameter brass wire was used. The sample was rigidly and symmetrically clamped. The contour cut location for the sample is marked on Figure 1(a). The WEDM cut progressed smoothly until the substrate location where the cutting speed slowed down due to the change in the thickness of the cut. The cutting speed through the deposit and substrate of the sample was about 0.3 mm/min and 0.05 mm/min respectively. The surface displacement profile of both cut halves of the sample was captured with a Zeiss Contura g2 CMM. For this purpose a 3-mm-diameter touch probe was used: and after defining the measurement plane and axis, a spacing of 0.5 mm used between the individual measurement points as well as from the perimeter, in both directions on the sample surface.

The displacement data of both cut surfaces/halves of the sample were post processed for data aligning, cleaning, flattening and smoothing using Matlab [25]. The data smoothing was performed with a cubic spline of knot spacing of 5.5 mm for both X & Y directions. The surface displacement data for this sample showed a smooth variation so a relatively large spline knot spacing could be used. A cubic spline function yields better fitting/smoothing than a quadratic function, for example. The finite element (FE) model was built from the measured perimeter of the sample. An 8-node brick element (C3D8R) of the Abaqus software was selected. The mesh size of the FE model was set to be uniform on the cut surface: *i.e.*, 0.5 mm. The smoothed displacement data with a reverse sign were then applied as the displacement boundary conditions to the model surface. Constraints were applied to the model to avoid rigid body motion. A linear-elastic FE analysis with the bulk material properties (as per ASM

Aerospace Specification Metals, Inc.) was performed to obtain the stress results: modulus of elasticity $E = 114$ GPa; Poisson's ratio $\nu = 0.342$.

For numerical simulation, a constant, orthotropic, inherent strain was calibrated on the observed part distortion, and the application was done layer-by-layer according to the mechanical layer equivalent approach [26]. A spatial discretization similar to the contour method FE model was used, except that the mesh chosen was slightly coarser and the theoretical symmetry of the geometry was used to model only half of the sample. The smallest elements were $2 \times 2 \times 2$ mm³ and the coarsest $10 \times 10 \times 2$ mm³, as the deposited layer thickness was 2 mm. A linear transient simulation with the sleeping elements was performed. In this approach there is no adding of the elements to the model matrix during the simulation, but rather the elements are given a negligible stiffness until “woken up” by the depositing of their layer. This approach has clear advantages when simulating the processes in which the only controlled quantity is the volume of the deposited material over time. Indeed in WFAM, the key controlled quantity is the material flux and the thickness of a layer. In case a workpiece deforms in the build-direction during a WFAM process, the next layer deposited will tend to follow this contour. A sleeping-element-approach is a way to approximate this with a low modelling effort. An elasto-plastic material model was used to simulate the stress field.

The above approach is a rapid and robust method, although likely less accurate than the higher fidelity thermo-mechanical approaches. The current approach is of much greater value to industry as it does not require the same costly material data and the modelling effort or run time. Also it does not require knowledge of the process parameters such as speed, power, etc.

Results

The averaged surface displacement profile of the Ti-6Al-4V sample is shown in Figure 3. The figure shows the relaxed surface contours as a consequence of the stress relief after cutting. The substrate of the sample was excessively pre-heated near the interface and therefore high displacements are seen in this region, reflecting a high level of residual stress. For spline smoothing a rectangular grid of the data was used. Therefore the averaged displacement data was in a rectangular grid. The data shown in Figure 4

were carefully extracted from this grid. The plotted data are up to the top of the deposit, however the round profile of the deposit top and wavy profile of the deposit sides could not be extracted precisely.

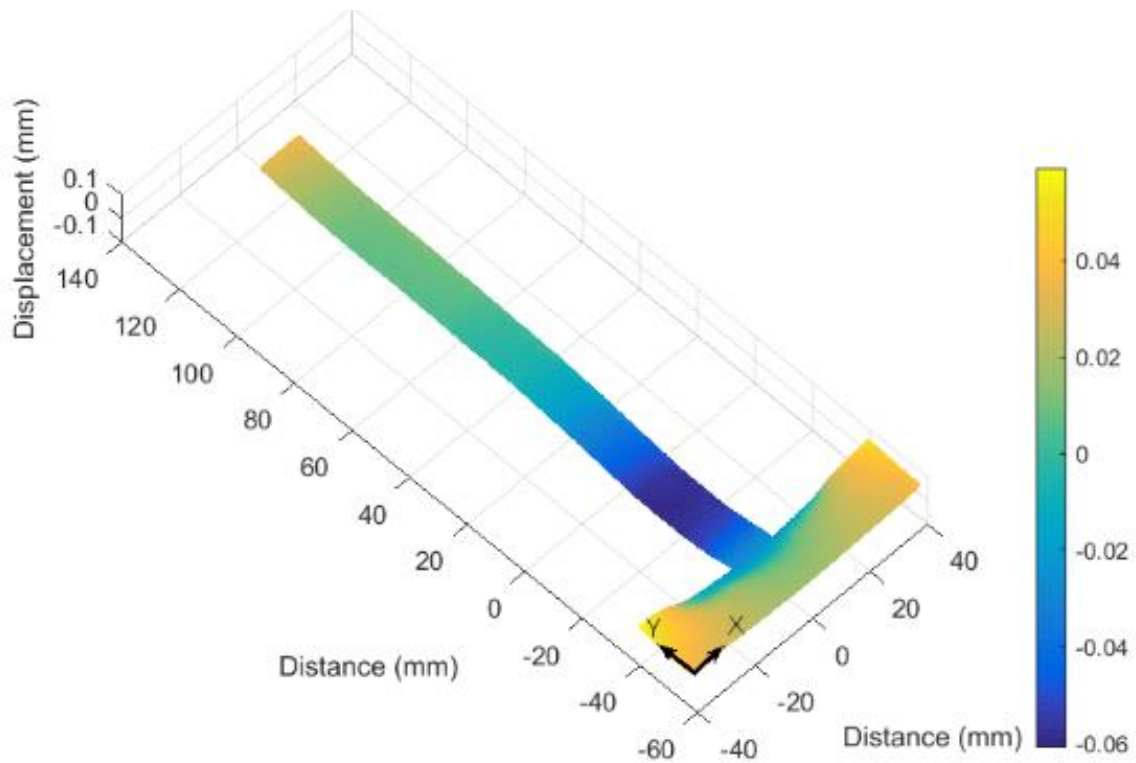


Figure 3. Averaged surface displacement profile of the sample

The contour stress map for the sample is shown in Figure 4. The highest tensile residual stress is seen in the substrate near to the root of the deposit, which occurred due to pre-heating of the sample substrate. Figure 5 illustrates these locations. The peak compressive residual stress is also seen in the substrate, below the tensile stress region. As a whole the tensile residual stress was accumulated near to the root of the deposit (*i.e.*, around the interface of the substrate and the deposit).

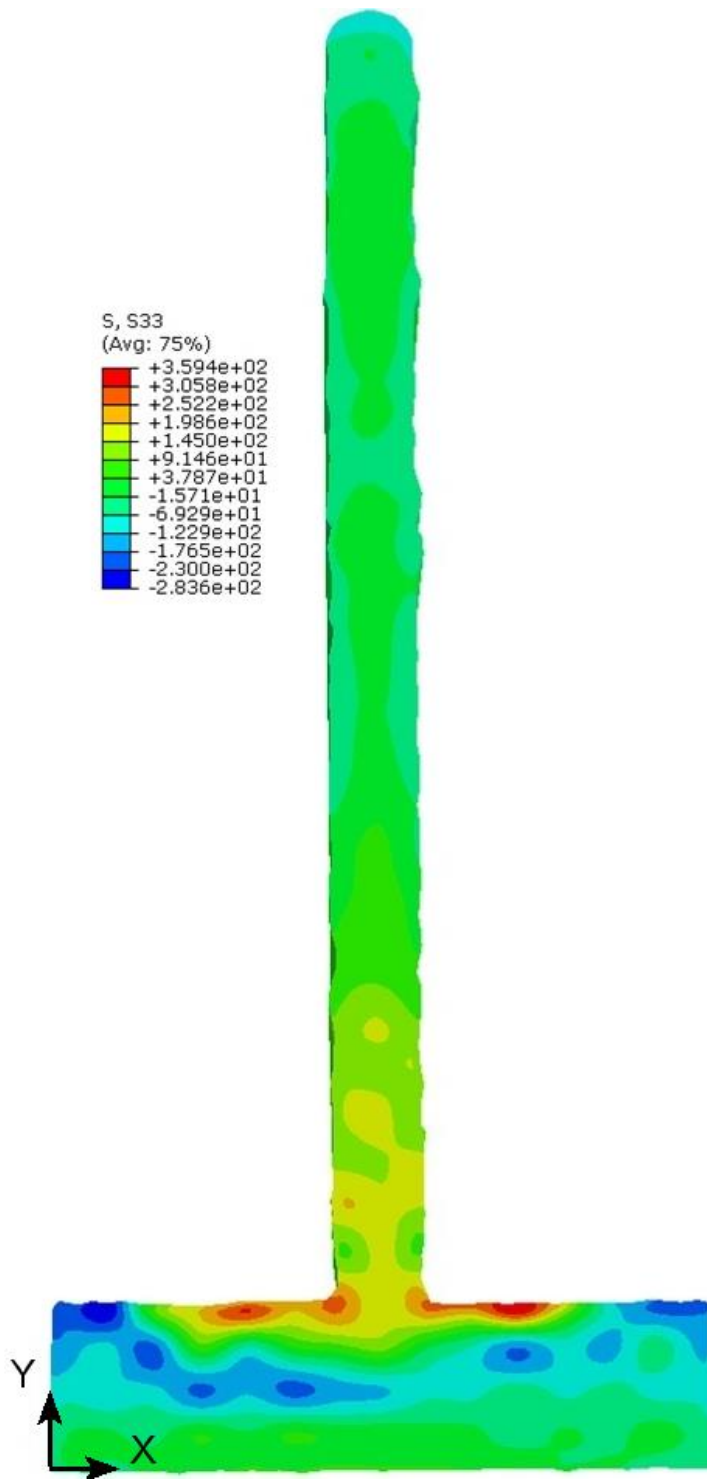


Figure 4. Contour stress map of WFAM titanium (Ti-6Al-4V) sample (Stress values are in MPa)

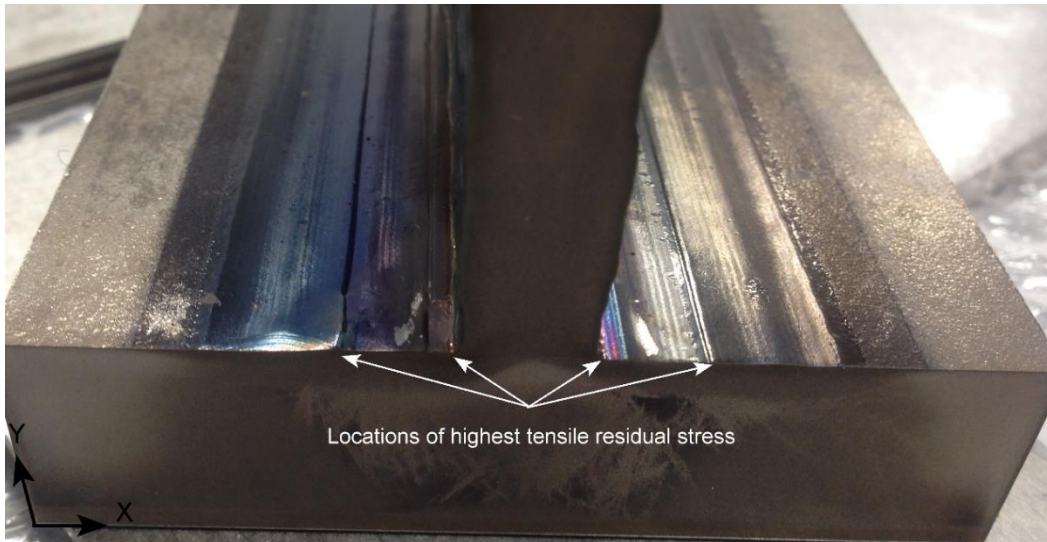


Figure 5. Locations of the highest tensile residual stress in the sample (Note: The colour of the WEDM cut surface shows the effect of the ultrasonic cleaning which removed the debris deposited from the cutting chamber)

For a comparison of the stress distribution in the sample, a number of lines/locations were identified as shown in Figure 6.

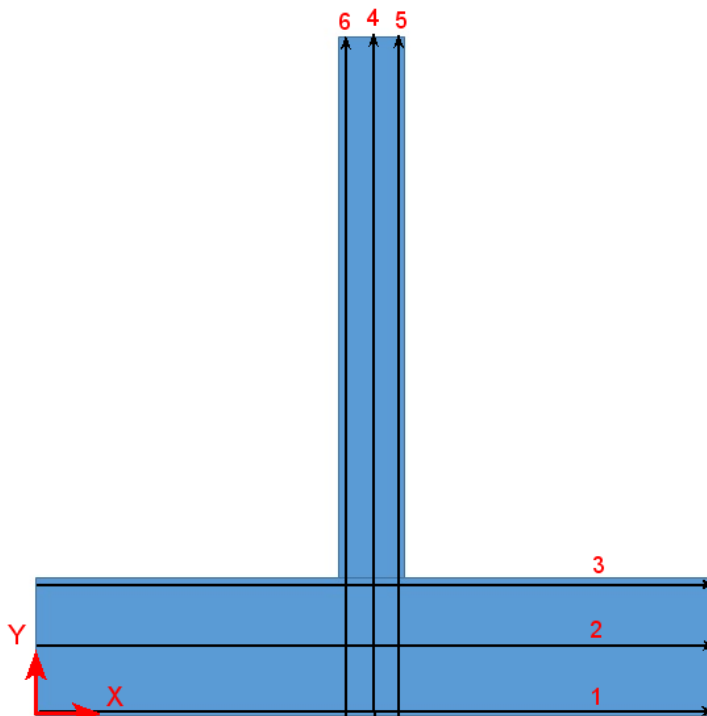


Figure 6. Locations and directions of stress line profiles for the sample (Diagram not to scale)

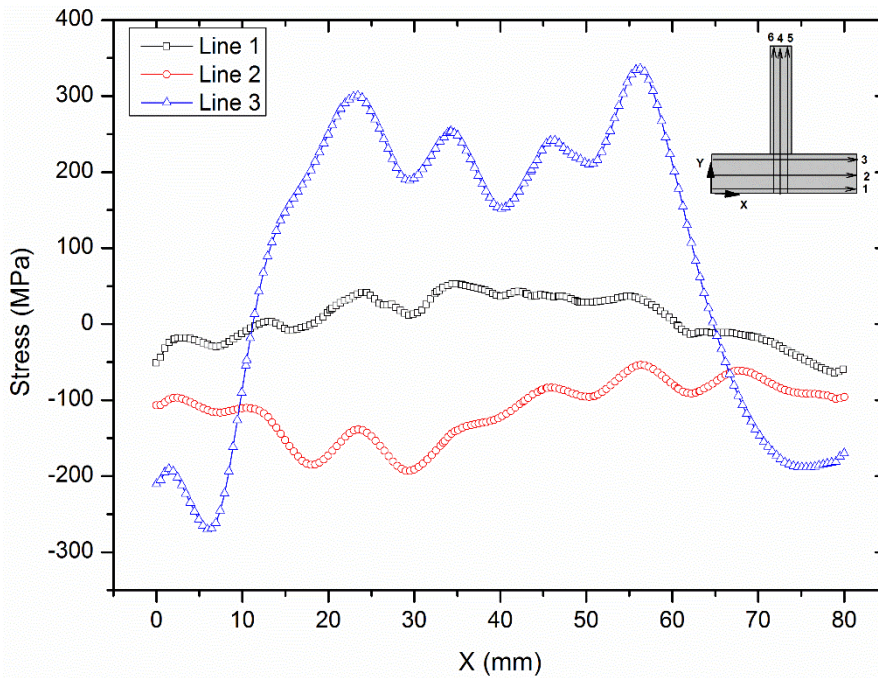
The axis for the lines drawn in Figure 6 is as below:

- | | |
|--|--|
| <u>Line 1</u> : along X-axis & at Y = 1 mm; | <u>Line 2</u> : along X-axis & at Y = 10 mm; |
| <u>Line 3</u> : along X-axis & at Y = 19 mm; | <u>Line 4</u> : along Y-axis & at X = 40 mm; |

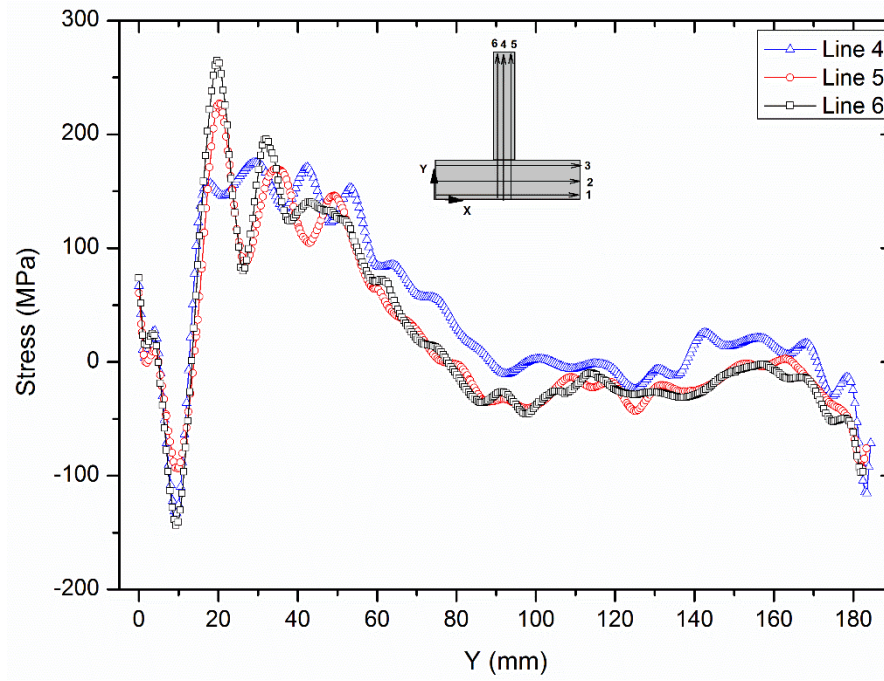
Line 5: along Y-axis & at X = 45 mm;

Line 6: along Y-axis & at X = 35 mm

Figure 7(a) shows the stress line profiles for the sample along lines 1, 2 & 3 (as per Figure 6). These lines show the stress distribution at the edges and middle of the substrate. We can see that in the substrate near to the deposit the stresses are tensile and high in magnitude whereas at the mid location of the substrate the stresses are mainly compressive. The stress distribution along line 3 mainly shows the influence of pre-heating the sample substrate. The stress line profiles for the sample along lines 4, 5 & 6 (as per Figure 6) are shown in Figure 7(b). These lines show the stress distribution in the whole sample, *i.e.*, from the bottom of the substrate to the top of the deposit, as well as at the middle and edges of the deposit. From this figure we can see that the tensile residual stress is high near to the region of the start of the deposit (*i.e.*, around the interface of the substrate and deposit: the central portion of line 3, and lines 4, 5 & 6 around Y = 19 mm). From the middle towards the top of the deposit the tensile residual stress decreases and becomes compressive (lines 4, 5, 6). The stress line profile at the mid-location of the deposit (line 4) is slightly different compared to the edge locations (lines 5 & 6): it is more tensile in the centre region compared to the edges. The stress line profiles however along the edges of the deposit (lines 5 & 6) are more or less identical.



(a)



(b)

Figure 7. Stress lines profile for the sample along (a) Line 1, 2 & 3, and (b) Line 4, 5 & 6, as shown in figure 6

The residual stress predicted with the numerical simulation (inherent strain-based method) is shown in Figure 8, which also gives a direct comparison with the contour method results. The numerical simulation showed peak tensile residual stress at the root of the deposit. The tensile residual stresses then reduced towards the top of the deposit and at the top of the deposit the stress state was compressive. A similar situation can be seen from the contour method results except for at the root of the deposit. The pre-heating the sample substrate and the heat affected zone of the initial deposited layers has altered the local residual stress state at & around of the root of the deposit, as confirmed by the contour method results, but this was not reflected in the modelling approach, hence the discrepancy. The numerical simulation results also showed that the top of the sample substrate has higher compressive residual stress as compared to the bottom. A similar case is seen for the contour method results, except for the top of the sample substrate which was affected by the excessive pre-heating and the heat-affected zone from the initial deposited layers.

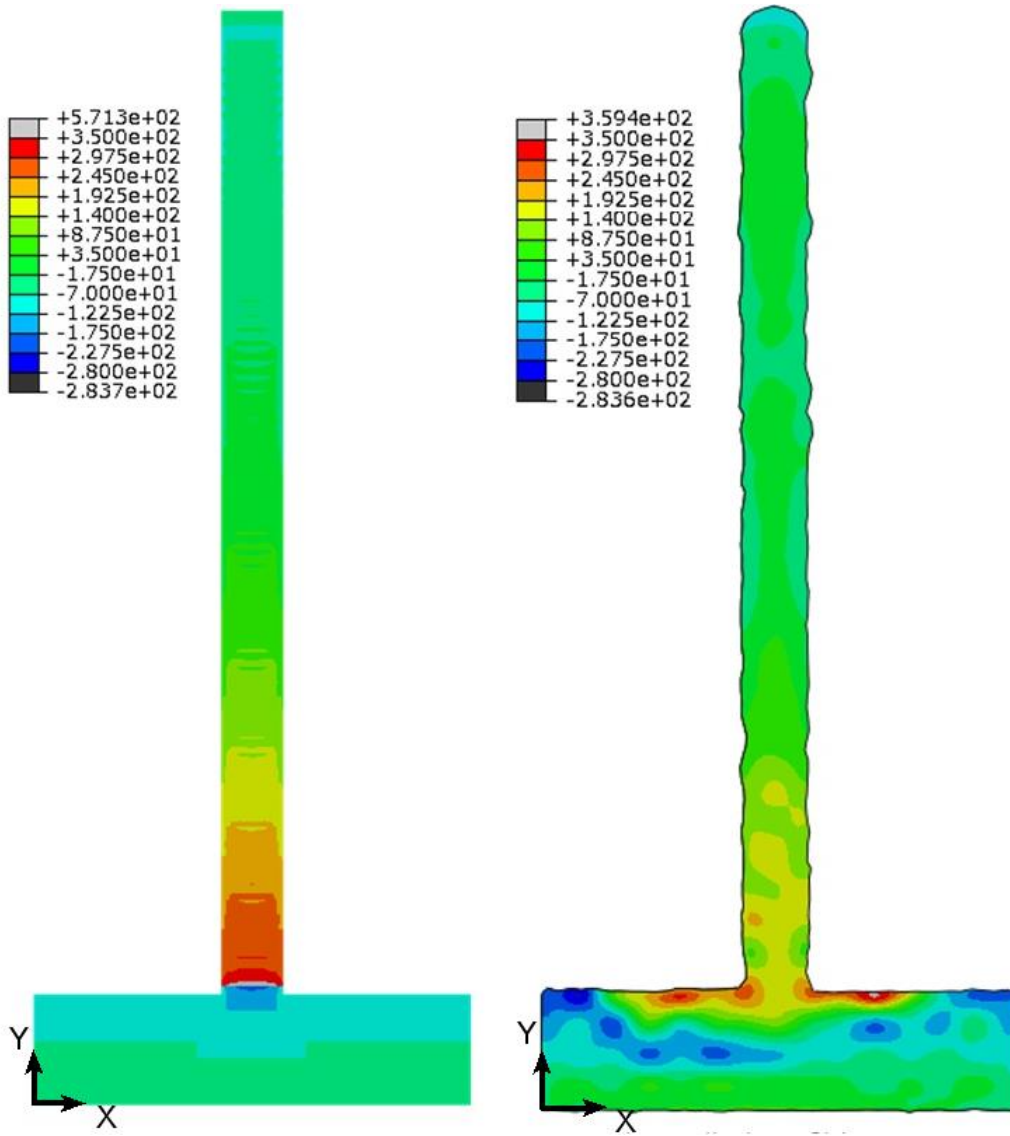
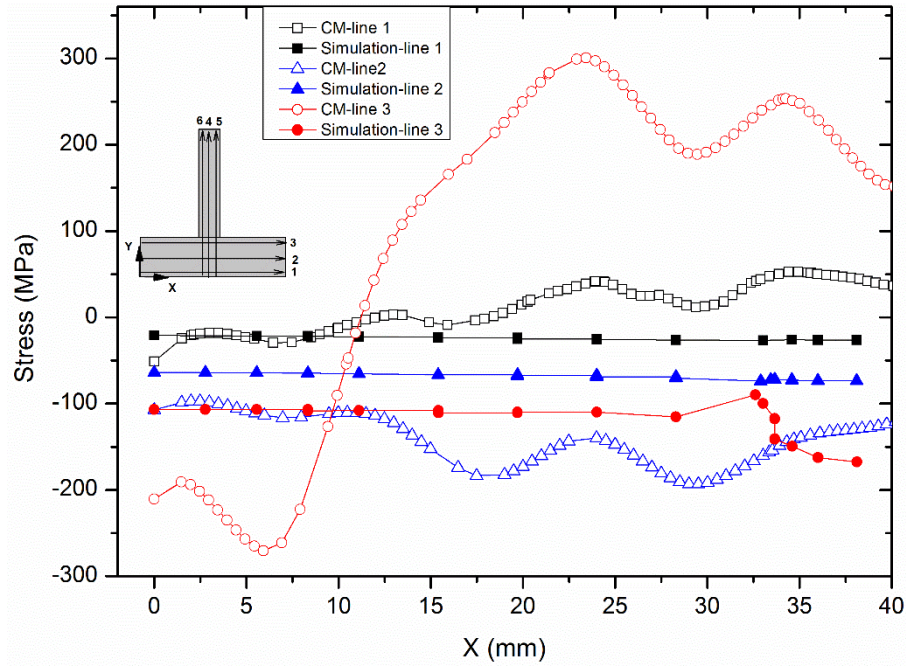
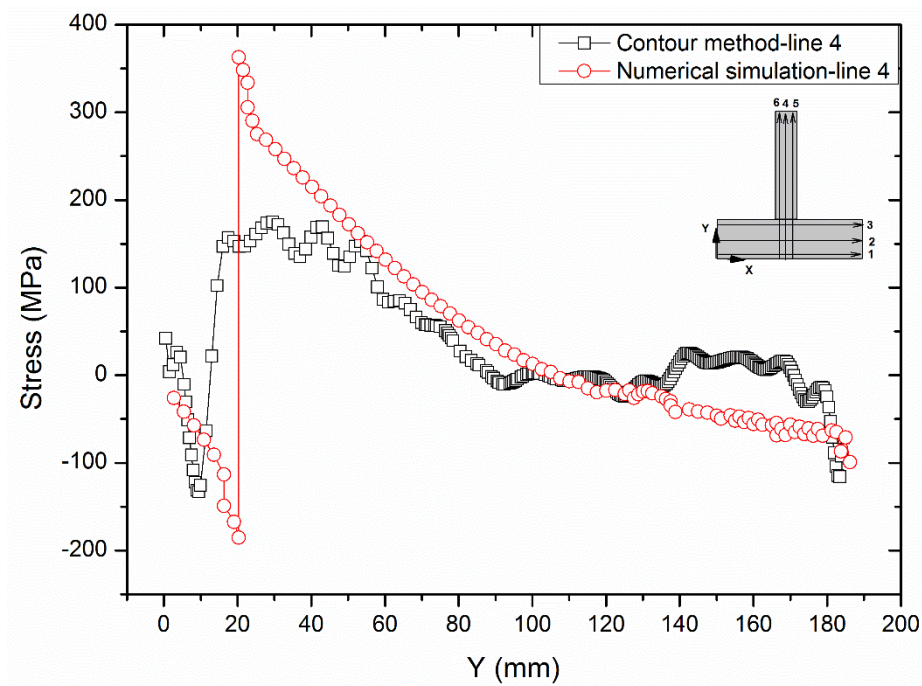


Figure 8. Predicted residual stress (left) compared to the measured contour method results (right). In both cases, the out-of-plane stress component σ_z is given. (Stress values are in MPa)

Figure 9 shows the predicted residual stress profiles along lines 1, 2, 3 & 4 (as per Figure 6), compared to the contour method results. Lines 1, 2 & 3 show the stress distribution in the substrate, from bottom (line 1) to top (line 3). The residual stress profile obtained from both approaches shows a discrepancy at the root of the deposit, where there is high variation between the stress magnitudes. Apart from the root of the deposit, a better correlation is achieved between two approaches. Note that due to symmetric stress profile of the simulation results only half data is plotted.



(a)



(b)

Figure 9. Comparison of residual stress line profiles between numerical simulation and contour method for (a) Line 1, 2 & 3, and (b) Line 4, as shown in figure 6

Discussion

The contour method measurement of the WFAM titanium (Ti-6Al-4V) sample showed a tensile residual stress magnitude of about 360 MPa around the interface of the

substrate and deposit. Moving towards the top of the deposit, at its centre location, the tensile residual stress decreased and becomes compressive (about -100 MPa). Highest compressive stress was seen in the substrate (up to about -280 MPa). Pre-heating the sample substrate at a higher temperature resultantly developed high tensile residual stresses in the substrate. However, the pre-heating may have eliminated the high tensile residual stresses in the initial deposited layers [5]. The gradient in the tensile residual stress and generation of the compressive residual stress towards the top of the deposit has also been noted previously [5]. A good correlation has been reported in the literature between the results obtained from the contour method and neutron diffraction in the deposit for the WFAM titanium alloy; however in the substrate the correlation was not good [5]. A numerical simulation predicted the tensile residual stress at and around the interface. In-addition, the effect of pre-heating passes on the residual stress distribution was predicted in electron-beam additively manufactured Ti-6Al-4V build plates [27]. In that study it was found that the tensile residual stresses have highly relaxed in the substrate after pre-heating, whereas a relatively small change in the stress distribution was achieved in the deposit. Neutron diffraction measurement of the wire + arc additively manufactured steel samples showed high tensile residual stresses at the interface of the deposit and substrate which were reduced after the application of rolling [28].

At the root of the deposit, there is a large discrepancy between the results obtained from the present numerical simulation (with the simple and robust inherent strain method) and the measurement. After investigation, this turned out to be due to the pre-heat pass performed in the real build. As it was not explicitly specified, and therefore was not accounted for in the simulation, which used a constant inherent strain throughout the entire part. Other than that, the distribution and even the magnitude of residual stress is well captured by the numerical simulation. It is seen that the peak tensile residual stress has shifted to the substrate from the root of the deposit after pre-heating. This also highlights the importance of pre-heating temperature and its subsequent impact on the residual stress distribution in the sample.

Conclusions

Residual stresses were estimated in a wire-feed additively manufactured titanium alloy component using numerical simulation (an inherent-strain-based approach) and

experimentally with the contour method. The sample was of T-shape geometry and the deposit was made on a titanium substrate. The key conclusions drawn from this study are as follows:

- The contour method measurement showed that the wire-feed additive manufacturing of the titanium alloy component caused high tensile residual stress at and around the interface between the substrate and deposit. High compressive residual stress was seen deeper in the substrate.
- The overall correlation of numerical simulation with the contour method was found to be satisfactory for certain industrial applications, where speed and robustness are more important than precision.
- Numerical prediction and the contour method measurement did not agree well locally at and near the interface of the substrate and deposit. This is due to the pre-heating of the sample substrate, which was not accounted for the simulation, as it used a constant inherent strain throughout the part.
- The pre-heating of the sample substrate developed peak tensile residual stress (about 360 MPa) in the substrate at near the edge of the start location of the deposit, which was measured by the contour method. On the other hand, the pre-heating may have reduced the magnitude of the tensile residual stress in the deposit.

Acknowledgements

The authors would like to thank Fred Carter and colleagues at Sciaky for providing the WFAM sample. We are also thankful to Steve Damms at The Institute for Advanced Manufacturing and Engineering, Coventry University, for his help with the WEDM. M. E. Fitzpatrick is grateful for funding from the Lloyd's Register Foundation, a charitable foundation helping to protect life and property by supporting engineering-related education, public engagement and the application of research.

References

- [1]. Dutta B, Froeas FH. The additive manufacturing (AM) of titanium alloys. *Met Powder Rep.* 2017;72:96-106.
- [2]. Levy LN, Schindel R, Kruth JP. Rapid manufacturing and rapid tooling with layer manufacturing (LM) technologies, state of the art and future perspectives. *CIRP Annals Manuf Technol.* 2003;52:589-609.

- [3]. Li P, Warner DH, Fatemi A, et al. Critical assessment of fatigue performance of additively manufactured Ti-6Al-4V and perspective for future research. *Int J Fatigue*. 2016;85:130-143.
- [4]. DebRoy T, Wei HL, Zuback JS, et al. Additive manufacturing of metallic components-Process, structure and properties. *Progr Materi Sci*. 2018;92:112-224.
- [5]. Martina F, Roy MJ, Szost BA, et al. Residual stress of as-deposited and rolled wire + arc additive manufacturing Ti-6Al-4V components. *Mater Sci Technol*. 2016;32:1439-1448.
- [6]. Baufeld B, Brandl E, van der Biest O. Wire based additive layer manufacturing: comparison of microstructure and mechanical properties of Ti-6Al-4V components fabricated by laser-beam deposition and shaped metal deposition. *J Mater Process. Technol*. 2011;211:1146-1158.
- [7]. Ding D, Pan Z, Cuiuri D, et al. Wire-feed additive manufacturing of metal components: technologies, developments and future interests. *Int J Adv Manuf. Technol*. 2015;81:465-481.
- [8]. Hönnige JR, Williams S, Roy MJ, et al. Residual stress characterization and control in the additive manufacture of large scale metal structures. *Mater Res Proc*. 2016;2:455-460.
- [9]. Szost BA, Terzi S, Martina F, et al. A comparative study of additive manufacturing techniques: residual stress and microstructural analysis of CLAD and WAAM printed Ti-6Al-4V components. *Mater Des*. 2016;89:559-567.
- [10]. Martina F, Colegrove PA, Williams SW, et al. Microstructure of interpass rolled wire + arc additive manufacturing Ti-6Al-4V components. *Metall Trans A*. 2015;46:6103-6118.
- [11]. Denlinger E. Thermo-mechanical model development and experimental validation of metallic parts in additive manufacturing [dissertation]. Pennsylvania: The Pennsylvania State University; 2015.
- [12]. Fujimoto T. A method for analysis of welding residual stresses and deformations based on the inherent strain method. *J Jpn Weld Soc*. 1970;39:236-252.
- [13]. Ueda Y, Fukuda K, Nakacho K, et al. A new measuring method of residual stresses with the aid of finite element method and reliability of estimated values. *Trans JWRI*. 1975;4:123-131.

- [14]. Ueda Y, Yuan MG. A predicting method of welding residual using source of residual stress (Report III). Trans JWRI. 1993;22:157-168.
- [15]. Ahmad B, Van-der-Veen SO, Fitzpatrick ME, et al. Residual stress evaluation in selective-laser-melting additively manufactured titanium (Ti-6Al-4V) and inconel 718 using the contour method and numerical simulation. Add Manuf. 2018;22:571-582.
- [16]. Prabhakar P, Sames WJ, Dehoff R, et al. Computational modelling of residual stress formation during the electron beam melting process for Inconel 718. Addit Manuf. 2015;7:83-91.
- [17]. Prime MB. Cross-sectional mapping of residual stresses by measuring the surface contour after a cut. Eng Mater Technol. 2000;123:162-168.
- [18]. Ahmad B, Fitzpatrick ME. Residual stresses in ultrasonically peened fillet welded joints. Adv Mater Res. 2014;996:755-760.
- [19]. Ahmad B, Fitzpatrick ME. Analysis of residual stresses in laser-shock-peened and shot-peened marine steel welds. Metall Mater Trans A. 2017;48:759-770.
- [20]. Ahmad B, Fitzpatrick ME. Minimization and mitigation of wire EDM cutting errors in the application of the contour of residual stress measurement. Metall Mater Trans A. 2016;47:301-313.
- [21]. Hosseinzadeh F, Traore Y, Bouchard PJ, et al. Mitigating cutting-induced plasticity in the contour method (Part 1, experimental). Exp Mech. 2016;94-95:247-25.
- [22]. Muransky O, Hamelin CJ, Hosseinzadeh F, et al. Evaluation of self-equilibrium cutting strategy for the contour method of residual stress measurement. Int J Pressure Ves Pipe. 2017. DOI: 10.1016/j.ijpvp.2017.04.002.
- [23]. Toparli MB, Fitzpatrick ME, Gungor S. Determination of multiple near-surface residual stress components in laser peened aluminium alloy via the contour method. Metall Mater Trans A. 2015;46:4268-4275.
- [24]. Zhang J, Wang X, Paddea S, et al. Fatigue crack propagation behaviour in wire + arc additive manufactured T-6Al-4V: effects of microstructure and residual stress. Mater Des. 2016;90:551-561.
- [25]. Johnson G. Residual stress measurement using contour method [dissertation]. Manchester: The University of Manchester; 2008.
- [26]. Keller N, Ploshikhin V. New method for fast predictions of residual stress and distortion of AM parts. Annu Int Solid Freeform Fab Symp. 2014:1229-1237.

- [27]. Cao J, Gharghoury MA, Nash P. Finite-element analysis and experimental validation of thermal residual stress and distortion in electron beam additive manufactured Ti-6Al-4V build plates. *J Mater Process Technol.* 2016;237:409-419.
- [28]. Colegrove PA, Coules HE, Fairman J, et al. Microstructure and residual stress improvement in wire and arc additively manufactured parts through high pressure rolling. *J Mater Process Technol.* 2013;213:1782-1791.

Figure 1. Wire feed additively manufactured titanium (Ti-6Al-4V) sample (a) Photo; & (b) Dimensions of the sample cut surface (all dimensions are in mm)

Figure 2. Schematic of clamping arrangement used during additive manufacturing

Figure 3. Averaged surface displacement profile of the sample

Figure 4. Contour stress map of WFAM titanium (Ti-6Al-4V) sample (Stress values are in MPa)

Figure 5. Locations of the highest tensile residual stress in the sample (Note: The colour of the WEDM cut surface shows the effect of the ultrasonic cleaning which removed the debris deposited from the cutting chamber)

Figure 6. Locations and directions of stress line profiles for the sample (Diagram not to scale)

Figure 7. Stress lines profile for the sample along (a) Line 1, 2 & 3, and (b) Line 4, 5 & 6, as shown in Figure 6

Figure 8. Predicted residual stress (left) compared to the measured contour method results (right). In both cases, the out-of-plane stress component σ_z is given. (Stress values are in MPa)

Figure 9. Comparison of residual stress line profiles between numerical simulation and contour method for (a) Line 1, 2 & 3, and (b) Line 4, as shown in figure 6